

Received Date: 10<sup>th</sup> November, 2025

Revision Date: 15<sup>th</sup> December, 2025

Accepted Date: 28<sup>th</sup> January, 2026

# Wireless Power Transfer through Inductive Coupling

Apekshya Shakya<sup>1\*</sup>, Bipin Prasad Devkota<sup>2</sup>, Purshottam Thakur<sup>3</sup>, Manish Bhattarai<sup>4</sup>

<sup>1</sup>Dept of Electrical Engineering, Pulchowk Campus, TU, Nepal. Email: 077bel009.apekshya@pcampus.edu.np

<sup>2</sup>Dept of Electrical Engineering, Pulchowk Campus, TU, Nepal. Email: 077bel019.bipin@pcampus.edu.np

<sup>3</sup>Dept of Electrical Engineering, Pulchowk Campus, TU, Nepal. Email: 077bel030.purushottam@pcampus.edu.np

<sup>4</sup>Dept of Electrical Engineering, Pulchowk Campus, TU, Nepal. Email: 077bel023.manish@pcampus.edu.np

**Abstract**— This paper proposes the wireless power transfer (WPT) through inductive coupling (IC). WPT can be described as the transfer of electrical energy from the source to the electrical load without using conductors connecting between transmitter and receiver coil. This paper highlights significant studies on the short-range inductive coupling and challenging in achieving high efficiency and safety over long distances.

**Keywords** — WPT, IC, electromagnetism, magnetically coupled

## I. Introduction

Wireless power transfer (WPT) is the technology that transfer electrical energy from the source to the electrical load without using the electrical conductors connecting between transmitter coil and receiver coil.[1] In 1890s Nikola Tesla first introduced the concept of WPT where he demonstrated a resonant transformer coil called Tesla coils [2]. However, due to the certain restriction, the development of WPT technology was left unfinished without thorough research [3].

WPT research has become an important topic among researchers, scientists and engineers. In 2007, a group of researchers from MIT did research on WPT using a pair of resonators that magnetically coupled and managed to power a light bulb of 60W over distances exceeding 2 meters with an efficiency of around 40% [4]. Using the principle of electromagnetic induction, WPT works on the concept of a primary coil generating a certain amount of magnetic field and a secondary coil being within that field so current is induced within its coils. This results in a relatively limited range, as generating a strong enough electromagnetic field requires a generous amount of power.

The recent advancements and model projects on the wireless transfer have demonstrated the real-world viability of wireless power charging. Some significant examples include deployments in California for BMW vehicles,

Oslo's wireless taxi charging stations, and South Korea's dynamic charging infrastructure for buses in Gumi. These implementations have achieved efficiency levels of 85–92% during stationary charging and 80–88% under dynamic conditions, showcasing the practicality as well as enhancing the reliability and efficiency of this technology [5]. Further exploring and expanding on these, this research focuses on the design and development of an efficient wireless charging system for inductive coupling, contributing to the global transition toward cleaner, sustainable and effective technology.

The main objective of this research is to focus on the study of wireless power transfer technology. The idea of wireless charging is to transfer power from the power grid to the load completely contact less. There are various concepts of contact-less energy transfer such as microwave, light, capacitive, inductive, radiative, etc.; however, inductive power transfer among them is the preferred technology for vehicular application. This research aims to explore various WPT technologies and innovations such as assessing potential future applications across electronics industries, IOT, transportation, etc.

## II. Materials and Methods

Power transfer occurs through magnetic flux coupling between two coils, known as inductive power transfer (IPT). This method is simple to use and suitable for transmitting high power, making it ideal for charging electric vehicles. [13]

Magnetic induction has long been used in transformers where coils are coupled through a magnetic core. However, when coils are separated by air, power can still be transferred wirelessly for EV charging. The efficiency of IPT depends on factors like air gap distance, coil size, and alignment. [13]

To improve this system, the magnetic gear wireless power transfer (MGWPT) method was developed. It uses coils and capacitors that work at the same resonant frequency

\* Corresponding Author

to transfer energy efficiently, even with weak magnetic coupling. This system also allows more flexibility in coil placement. [1]

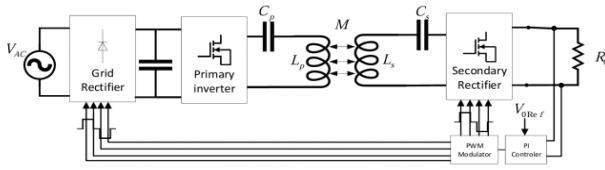


Fig.1 WPTS Architecture

The Magnetic Gear power transfer circuit consists of transmitter coil, receiver coil, power source, resonant circuit, rectifier circuit, voltage regulator and load as shown in Fig.1. In resonant circuit, To enhance power transfer capability, the primary and secondary coils are tuned to the same frequency. This increases the power efficiency of the circuit.

#### A. Design Parameters of Coil and Circuits

a. *Basics of Electromagnetism:* The basics of electromagnetism are derived from Maxwell's equations, both in time

independent and time-dependent cases. The four Maxwell equations are as follows:

$$\oint \vec{E} \cdot d\vec{l} = -\frac{\partial \vec{B}}{\partial t} \quad (\text{Faraday's Law}) \quad (1)$$

$$\oint \vec{H} \cdot d\vec{l} = \vec{j} + \frac{\partial \vec{D}}{\partial t} \quad (\text{Ampere's Law}) \quad (2)$$

$$\oint \vec{D} \cdot d\vec{s} = \rho_v \quad (\text{Gauss's Law for Electricity}) \quad (3)$$

$$\oint \vec{B} \cdot d\vec{s} = 0 \quad (\text{Gauss's Law for Magnetism}) \quad (4)$$

where E is electric field intensity, H is magnetic field intensity, D is displacement vector, B is magnetic flux density. There are four laws associated with the Maxwell: they are Faraday's law of electro-magnetism, Ampere's law, the third and fourth are Gauss laws for the electric and magnetic fields.

b. *Resistance and Skin Depth:* The dc resistance (R) is the wire resistance when the applied voltage is DC or low frequency AC, it can be written as a relationship between the resistivity (Rho) of the wire length (L), and cross-section region (A) as given:

$$R = \frac{\rho L}{A} \quad (5)$$

As the frequency rises, the current which charges distribution in the conductor will change from a consistent spread throughout the whole conductor volume to a surface distribution only (as shown in Fig.2), this phenomenon is

called the skin effect. Skin effect ( $\delta$ ) is the calculation of how the current distribution varies with frequency shifts. Also, the skin depth is defined as "the depth from the conductor's outer surface to a point where the current density is reduced 1/e (i.e. about 37 Percent) of its value at the surface" [7].

$$\delta = \sqrt{\frac{2\rho}{\omega\mu}} = \frac{1}{\sqrt{\pi f\mu\sigma}} \quad (6)$$

Where:  $\mu_0$  is the conductor's absolute magnetic permeability,  $f$  is the frequency of the current. [13]

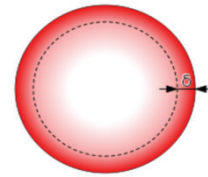


Fig.2 Skin Effect

c. *Resonance:* The electrical resonance happens in the electrical circuit at a certain frequency called resonant frequency ( $f_r$ ). At that frequency, an imaginary part of the impedances and the admissions of the circuit are equal so they cancel each other. The resonance of a circuit containing capacitors and inductors happens because the inductor's contracting magnetic field produces an electrical current in its windings which charges the capacitor and when discharging it creates an electrical current that builds the inductor's magnetic field. This process is continuously repeated, creating a resonant frequency [7]. The magnitude of the transfer function when the output is taken over the LCR series resistor R shown:

$$|H(\omega)| = \frac{|V_o(\omega)|}{|V_i(\omega)|} = \frac{R}{Z} = \frac{R}{\sqrt{R^2 + (\omega L - \frac{1}{\omega C})^2}} = \frac{\omega CR}{\sqrt{\omega^2 C^2 R^2 + (\omega^2 LC - 1)^2}} \quad (7)$$

It can be obtained:

$$\omega_0 = \sqrt{\omega_1 \omega_2} \quad (8)$$

That means for the LCR series circuit the resonance frequency is the geometric mean of a half-power frequencies. The resonance frequency of the RLC series circuit is calculated by:

$$f_r = \frac{1}{2\pi\sqrt{LC}} \quad [\text{Hz}] \quad (9)$$

d. *Coupling Factor:* The coupling factor (k) is a dimensionless value that defines the connection between the primary and secondary coils in a Wireless Power Transfer (WPT) system. A higher coupling factor indicates better power transfer efficiency, as it reduces magnetic flux losses and minimizes heating. Consider two types of coupling modes: tightly coupled and loosely coupled. In a tightly coupled circuit, the

transmitter ( $T_x$ ) and receiver ( $R_x$ ) coils are aligned with small air gap between them than the coil diameter. This configuration allows the receiver coil to capture most of the magnetic flux, efficiently converting it into electrical energy. While in loosely coupled systems, the distance between the transmitter ( $T_x$ ) and receiver ( $R_x$ ) coils exceeds the coil diameter. As a result, the magnetic flux is not fully transmitted. This occurs due to the larger air gap between the coils or a mismatch in their diameters, such as when the transmitter coil ( $T_x$ ) is larger than the receiver coil ( $R_x$ ) [8].

**B. Basic Realization of Resonant Inductive WPT System**

Inductive power transfer works by generating a magnetic field in the primary (transmitter) coil, which induces a current in the secondary (receiver) coil. The system is designed with a low-quality factor (less than 10) to ensure efficient energy transfer. Inductive charging is widely used for low-power devices like phones and electric toothbrushes because it is easy to implement, safe, and efficient over short distances. Fig.3 shows the basic diagram of an inductive power transfer (IPT) system [6-8].

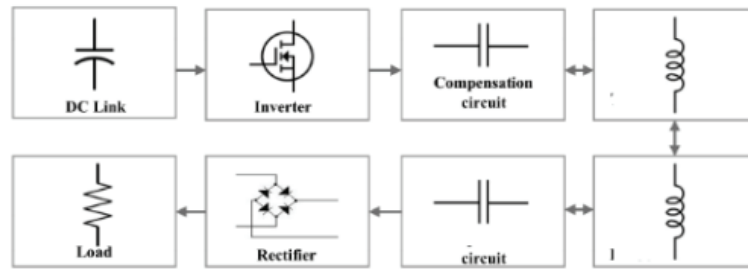


Fig.3: General diagram of IPT system

a. **Inverter:** The inverter is the first stage of the WPT system. It converts DC voltage from the power source into AC voltage. The frequency of the AC voltage depends on the input pulses applied to the inverter. The AC current flows through the primary coil, creating a magnetic field that induces a current in the secondary coil. There are two common types of inverters used in WPT systems: Half-bridge inverter and full-bridge inverter as shown in Fig.4 and Fig.5 respectively [9].

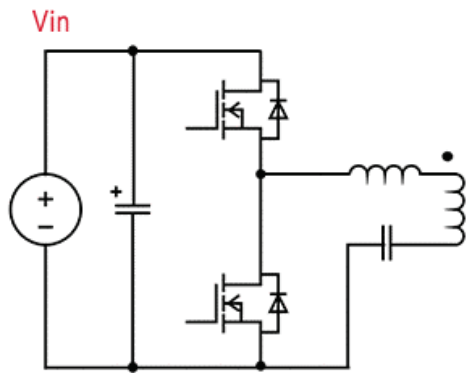


Fig.4(a) DC to AC half-bridge inverter circuit

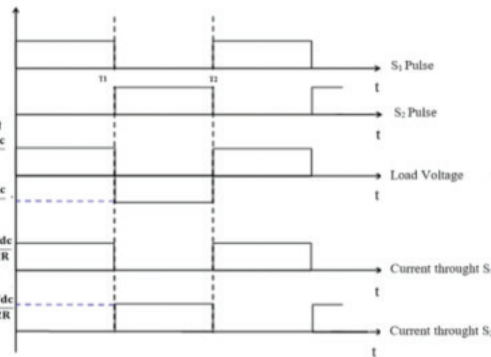


Fig.4(b) Load voltage and switches current in the half-bridge inverter

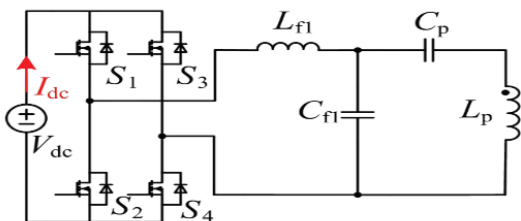


Fig.5(a) Circuit diagram of the full-bridge inverter

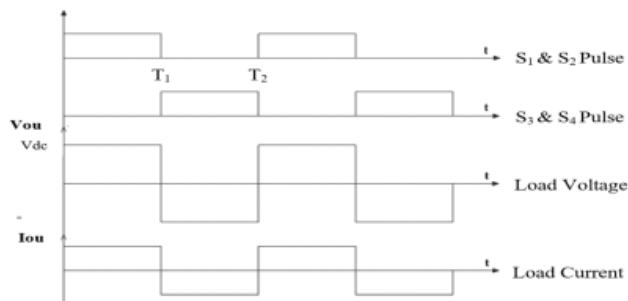


Fig.5(b) Load voltage and current in the Full-bridge inverter

*b. Inverter Switching Device:* Switching devices like transistors, MOSFET and IGBT are used in inverters to control the current flow. Two common types of transistors are used: MOSFET (Metal Oxide Semiconductor Field Effect Transistor) and IGBT (Insulated Gate Bipolar Transistor)

*c. Rectifier:* The rectifier is located on the receiver side of the WPT system. It converts the high frequency AC voltage from the receiver coil into DC voltage to power the load. A simple rectifier uses diodes to achieve this conversion. Fig.6 shows a basic rectifier circuit with a resistive load and a capacitive filter [10].

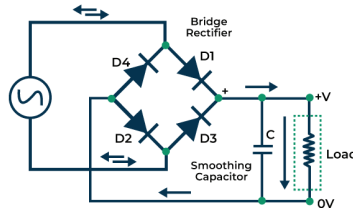


Fig.6 Rectifier circuit with resistive load and capacitive output filter

*d. Compensation Elements:* A compensation circuit is required in order to maximize the efficiency of the power transfer from the source to the load. Since the coils are used as an inductive element to coupling the transmitter stage with the receiver stage, then the compensation elements which should be used are capacitors. The compensation elements are connected in the transmitter stage ( $C_1$ ) and also in the receiver stage ( $C_2$ ) as shown in the Fig.7. There are four types of compensation topologies according to the connection type between the coils and the compensation element, series-series (SS), series-parallel (SP), parallel-series (PS), and parallel-parallel (PP) [9-11] as shown in Fig.7(a), 7(b) 7(c) and 7(d). The first word (letter) refers to the transmitter stage, while the second word refers to the receiver stage. The choosing of a certain topology rather than another depends on the particular application

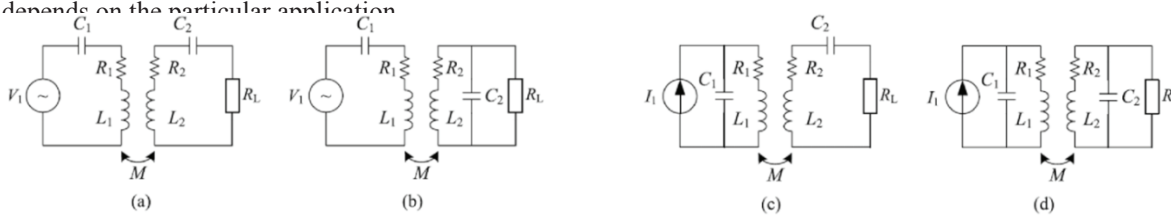


Fig 7 The basic topologies: Fig.7(a) SS, (b) SP, (c) PS and (d) PP

The SS topology is commonly used because it depends only on the self-inductance of the coils, making it less sensitive to misalignment between the transmitter and receiver coils [14].

*C. Calculation of Electrical Parameters for the WPT System*

The block diagram and components of the WPT system with the SS compensation element are illustrated in Fig.8.

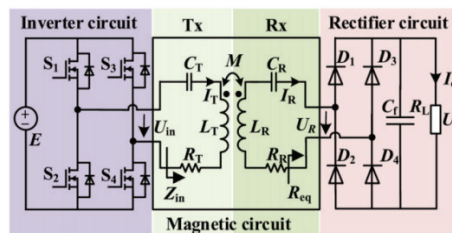


Fig.8 WPT system with SS compensation elements

The required output power ( $P_o$ ) calculation is based on the load requirements [10]. For a battery load, the equivalent resistance is calculated

$$R_{LB} = V_{out}^2 / P_{out} \tag{10}$$

The equivalent resistance ( $RL$ ) seen by the receiver coil is calculated as:

$$R_L = \frac{8V^2_{out}}{\pi^2 P_{out}} \quad (11)$$

The RMS value of the secondary voltage and current are given by:

$$V_{s,rms} = \frac{2\sqrt{2}V_{out}}{\pi} \quad (12)$$

$$I_{s,rms} = V_{s,rms} / R_L \quad (13)$$

The primary current is calculated as

$$I_{p,rms} = P_{in} / V_{p,rms} \quad (14)$$

The mutual inductance (M) between the coils is calculated using:

$$L_{Rx} = q_{Rx} \cdot R_L / \omega_r \quad (15)$$

The coupling factor can be calculated as:

$$k < \frac{1}{qs} \sqrt{1 - \frac{1}{4q^2}} \quad (16)$$

The transmittance coil inductance can be calculated as:

$$LT_x = \frac{M^2}{LT_x \cdot k^2} \quad (17)$$

Then after the above calculation of the parameters of the WPT system, the physical building of the coils are developed as shown in Fig.9.

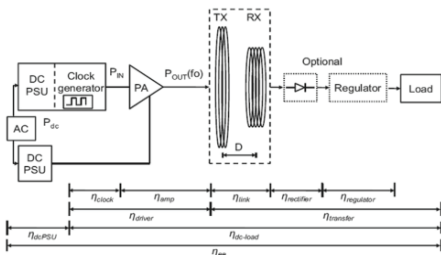


Fig.9 IPT systems architecture

**D. Displacement Flexibility**

The WPT system is very sensitive to alignments and the relative location between the coils of the transmitting (Tx) and receiving (Rx). In other words, the system efficiency deteriorates concerning a lateral or angular misalignment as illustrated in Fig.10[12].

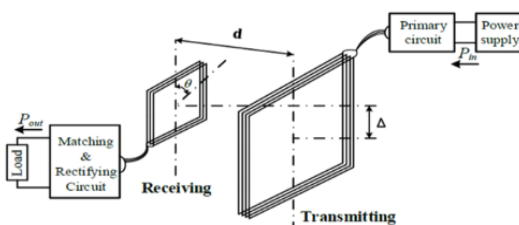


Fig.10 Misalignment of WPT systems

**E. Selecting Wire Type**

It needs special wire because high frequency causes problems with regular wire. "Litz wire" is made of many thin, insulated wires twisted together. This works better at high frequencies.

Table I

Best Wire Size for selected Frequency

Frequency Range	Wire Size	Thickness (mm)
50 kHz to 75 kHz	38 AWG	0.617

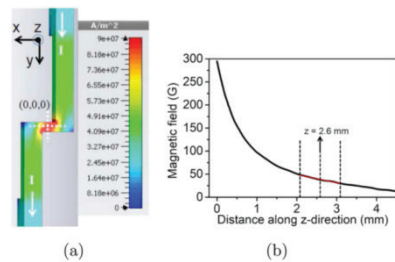


Fig.11 Regular Wire - Current stays near surface

Two coils are designed - one for transmitting power and other for receiving power. After testing different shapes, we chose circular coils as they work best.

Table II

Details of a) transmitter coil b) receiver coil

Parameter	Value
Number of turns	28
Coil Inductance	275 μH
Coil Resistance	1 Ω
Coil Size	40 cm diameter

Parameter	Value
Number of turns	26
Coil Inductance	300 μH
Coil Resistance	0.1 Ω
Coil Size	40 cm diameter

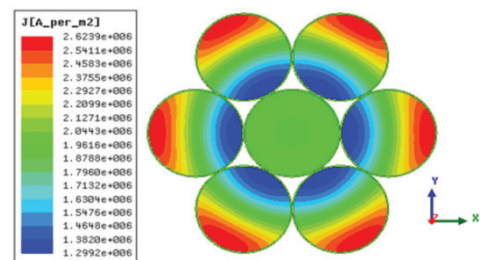


Fig: Litz Wire - Current spreads evenly

**F. Software Implementation: Simulation**

The simulation was conducted in MATLAB. It consists of several functional blocks, outlined as: Power Supply, Power Electronics Process, Battery Bank, Battery Status, output from the Battery and display unit which their performance on the simulation are given below:

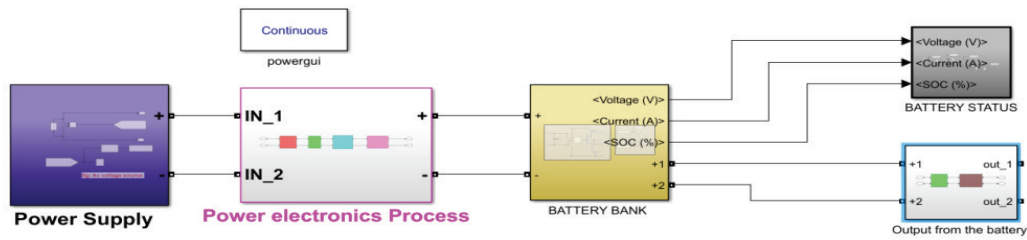


Fig.12 Overall Simulation Diagram

### G. Hardware Implementation

The main circuit consists of three major parts: the Oscillating Circuit, the Driving Circuit, and the Converter Circuit.

*Oscillating Circuit:* The circuit diagram of the oscillator is created in Proteus software, which consists of the 555 IC, a resistor, a capacitor and a DC voltage source. The circuit diagram of the oscillator is shown below:

*Driving Circuit:* Circuit The driver IC used in the driving circuit is the IR2110. This IC is used to drive both the high-side and the low-side MOSFETs. The input of the oscillating circuit is given to the driving circuit.

*Converter Circuit:* A half-bridge configuration is used in this project. Two MOSFETs are used, and the high-side MOSFET receives a 25V DC supply. The IR2110 driver provides gate signals to both MOSFETs, and the output of the MOSFETs is fed into the primary coil of the circuit.

*Primary Coil with Compensation Circuit:* Here, the PP LCC topology has been used for the compensation network. The LCC stands for one inductor and two capacitors. The PP stands for the parallel configuration of the inductor and capacitor.

*Complete Hardware Circuit Design in Proteus:* consisting of oscillator, IR2110, half bridge and primary coil, created in Proteus software, is shown below.

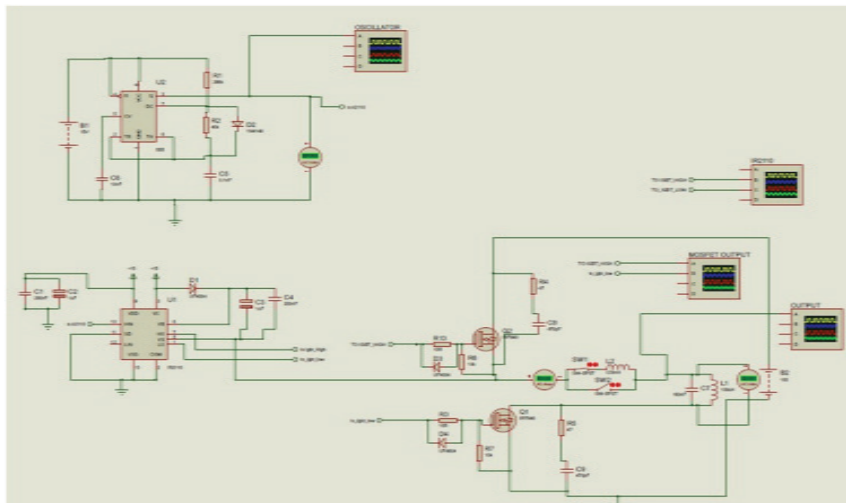


Fig.13 Complete Hardware Circuit Diagram in Proteus

### H. Applications of WPT Systems

WPT systems are used in a wide range of applications. In consumer Electronics, wireless charging pads used for smartphones, smartwatches, and other portable devices. In electric vehicles (EVs), wireless charging stations for EVs, both static (parked) and dynamic (in-motion) are used. Wireless power for implantable medical devices like pacemakers, reducing the need for invasive battery replacements. Wireless charging for robots and automated guided vehicles (AGVs) in manufacturing and logistics in industrial automation. Others like drones and other unmanned systems, enhancing their operational range and flexibility.[6]

### III. Result

Each circuit block in the simulation serves a specific purpose. However, the most significant results are obtained from the interaction between the primary and secondary circuits. The input signal supplied to the primary coil and the output signal received from the secondary coil is compared.

The waveform of the input signal applied to the primary coil is shown in Fig.14. This signal has a magnitude of approximately 829 volts and a frequency of 10 kHz. The waveform obtained from the secondary coil is shown in Fig.15. This output demonstrates the energy transfer efficiency and overall response of the inductive coupling system.

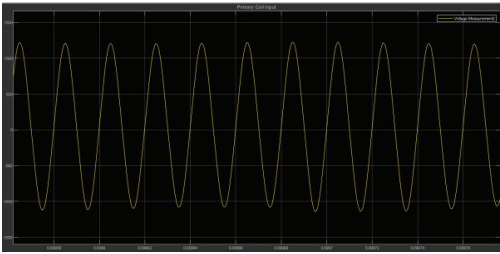


Fig.14 Input signal waveform applied to the primary coil.

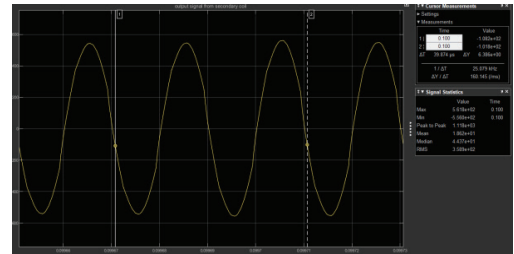


Fig.15 Output signal waveform measured from the secondary coil.

#### Hardware Implementation Results

The graphs from the simulation are displayed here. These graphs consist of the waveform of the oscillating, driving, converting, and output devices.

#### Proteus Simulation Result

- *Waveform of the Oscillating Circuit:* The output from the oscillating circuit is of 50 kHz. It is a square wave and is given as a PWM signal to the driving circuit.
- *Waveform of the Driving Circuit:* The 50 kHz–100 kHz PWM from the oscillating circuit is given to the driving circuit. It is observed that the high-side output of the IR2110 is not a perfect square wave.
- *Waveform of the Converting Circuit:* The half-bridge configuration is used. The output of the converting circuit is given to the primary coil.
- *Waveform of the Converting Circuit:* The half-bridge configuration is used. The output of the converting circuit is given to the primary coil.

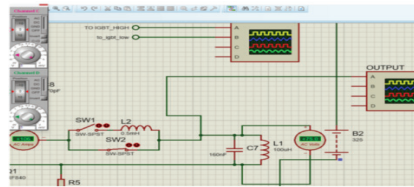


Fig.16 Waveform from the output circuit

#### Comparison without and with Compensation Circuit

Without the compensation network, the input and output voltages decreased.

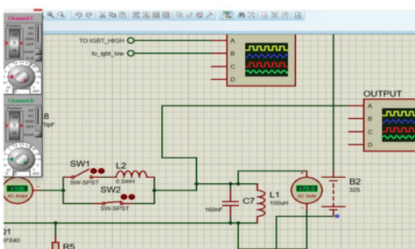


Fig.17 Circuit Without Compensation

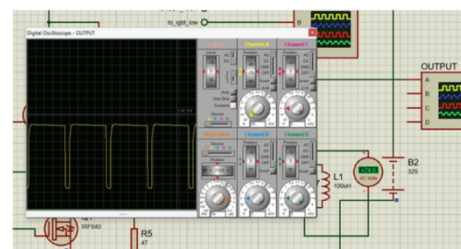


Fig.18 Waveform Without Compensation

With PP LCC compensation:

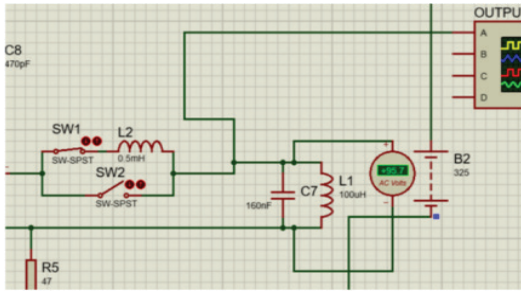


Fig.19: Circuit With LCC Compensation-1

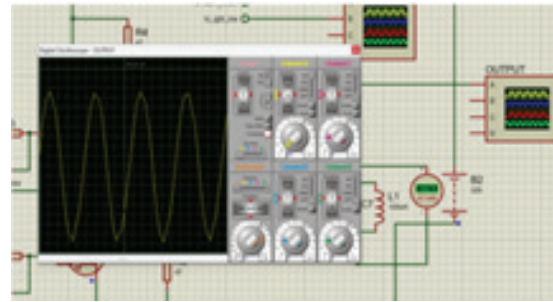


Fig.20: With LCC Compensation-2

The efficiency ( $\eta$ ) of a system is given by:

$$\eta = \frac{P_{out}}{P_{in}} \times 100\%$$

Where  $P = V \cdot I$  Therefore:

$$\eta = \frac{V_{out} I_{out}}{V_{in} I_{in}} \times 100\%$$

Table III  
Measured values

	$V_{in}$	$V_{out}$	$I_{in}$	$I_{out}$	Efficiency
5cm	33V	53V	33A	0.1mA	40%
10cm	33V	41V	33A	0.1mA	16%

Software Implementation Results in MATLAB

1. Without LCC

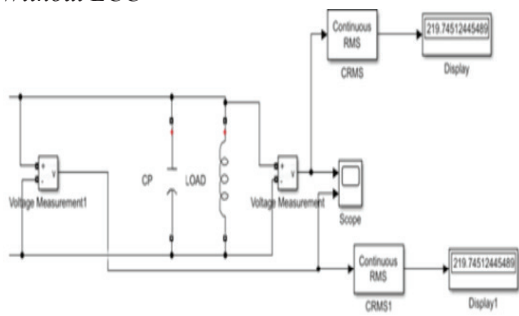


Fig.21 Simulation Circuit Without LCC-1

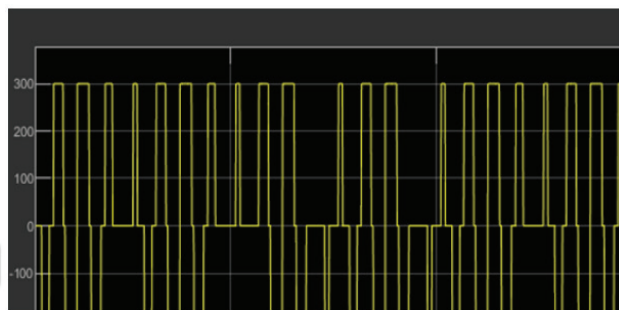


Fig.22 Simulated waveform without LCC-1

2. With LCC

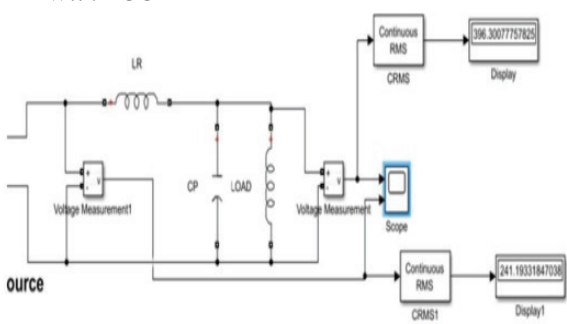


Fig.23 Simulation Circuit with LCC

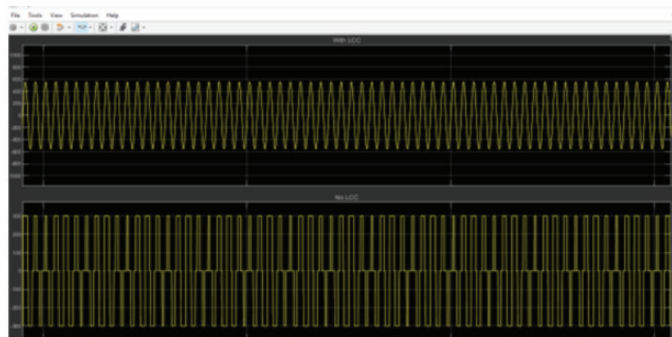


Fig.24 Simulated waveforms with LCC

Table IV:

Calculation of data taken from MATLAB

Parameter	Value
Primary winding inductance ( $L_1$ )	266.16 $\mu$ H
Primary winding resistance ( $R_1$ )	1m $\Omega$
Secondary winding inductance ( $L_2$ )	256.79 $\mu$ H
Secondary winding resistance ( $R_2$ )	1m $\Omega$
Mutual Inductance (M)	85.46 $\mu$ H
Primary capacitor ( $C_1$ )	105.74nF
Secondary capacitor ( $C_2$ )	109.69nF
Primary voltage ( $V_p$ )	829V
Primary current ( $I_1$ )	15A
Secondary Voltage ( $V_s$ )	400V
Secondary current ( $I_2$ )	1.4A

A. Resonant frequencies: *The resonant frequency of each tuned coil is calculated as:*

$$f = \frac{1}{2\pi\sqrt{LC}}$$

$$f_1 = \frac{1}{2\pi\sqrt{L_1 C_1}} = \frac{1}{2\pi\sqrt{(266.16 \times 10^{-6})(105.74 \times 10^{-9})}} \approx 30000.54 \text{ Hz} \approx 30.00 \text{ kHz}$$

$$f_2 = \frac{1}{2\pi\sqrt{L_2 C_2}} = \frac{1}{2\pi\sqrt{(256.79 \times 10^{-6})(109.69 \times 10^{-9})}} \approx 29988.00 \text{ Hz} \approx 29.99 \text{ kHz}$$

Both coils are therefore tuned very near **30 kHz**.

B. Coupling coefficient: *The coupling coefficient is*

$$k = \frac{M}{\sqrt{L_1 L_2}} = \frac{85.46 \times 10^{-6}}{\sqrt{(266.16 \times 10^{-6})(256.79 \times 10^{-6})}} \approx 0.3269 \approx 0.33$$

So the magnetic coupling is about **33%**.

B. Input and output powers (assume power factor  $\approx 1$ )

Real input power (approximate):

$$P_{in} = V_p I_1 = 829 \times 15 = 12435 \text{ W}$$

Real output power:

$$P_{out} = V_s I_2 = 400 \times 1.4 = 560 \text{ W}$$

Power lost (difference):

$$P_{loss} = P_{in} - P_{out} = 12435 - 560 = 11875 \text{ W}$$

$$\eta = \frac{P_{out}}{P_{in}} \times 100\% = \frac{560}{12435} \times 100\% \approx 4.503\% \text{ (approx.)}$$

E. Load and reflected impedance (ideal transformer approximation)

Load impedance at the secondary:

$$Z_{load} = \frac{V_s}{I_2} = \frac{400}{1.4} \approx 285.714 \Omega$$

$$\frac{N_1}{N_2} \approx \frac{V_p}{V_s} = \frac{829}{400} \approx 2.0725$$

$$Z_{ref} = \left(\frac{N_1}{N_2}\right)^2 Z_{load} \approx (2.0725)^2 \times 285.714 \approx 1227.22 \Omega$$

If the source had negligible series impedance, the ideal-model primary current would be

$$I_{1,ideal} = \frac{V_p}{Z_{ref}} \approx \frac{829}{1227.22} \approx 0.6755 \text{ A}$$

F. Coil copper loss (approximate)

Primary copper loss (using measured  $I_1 = 15 \text{ A}$  and  $R_1$ ):

$$P_{R1} = I_1^2 R_1 = 15^2 \times 1 \times 10^{-3} = 225 \times 10^{-3} = 0.225 \text{ W}$$

(Secondary copper loss similarly

$P_{R2} = I_2^2 R_2 = 1.4^2 \times 1 \times 10^{-3} \approx 0.00196 \text{ W}$ .) These resistive losses are *negligible* compared to the measured input/output power discrepancy.

Table V  
Computed Values

Parameter	Value
Primary resonant frequency	$f_1 \approx 30.00 \text{ kHz}$
Secondary resonant frequency	$f_2 \approx 29.99 \text{ kHz}$
Coupling coefficient	$k \approx 0.3269$
Input power	$P_{in} = 12435 \text{ W}$
Output power	$P_{out} = 560 \text{ W}$
Efficiency	$\eta \approx 4.503\%$
Load impedance	$Z_{load} \approx 285.71 \Omega$
Reflected impedance	$Z_{ref} \approx 1227.22 \Omega$
Ideal primary current (from reflected load)	$I_{1,ideal} \approx 0.6755 \text{ A}$

#### IV. Discussion

The output voltage induced in the secondary coil depends on several interrelated factors such as coupling coefficient, coil alignment, distance between coils, and input excitation parameters. We verified our results from the simulation by comparing with mathematical calculations, testing different parameters, checking against known wireless power principles. From the obtained results, it is observed that the output voltage decreases as the distance between the coils increases. Consequently, the overall efficiency of wireless power transfer also decreases with increasing separation.

The low experimental efficiency can be attributed to several factors:

1. *Coil Alignment*: Proper alignment between the primary and secondary coils is crucial to achieve maximum magnetic coupling. Any misalignment significantly reduces the mutual inductance and transferred power.
2. *Input Voltage*: Increasing the input DC voltage or excitation amplitude enhances the magnetic field strength, which in turn increases the induced voltage at the receiver coil.
3. *Rate of Change of Magnetic Flux*: The induced electromotive force (EMF) in the secondary coil is directly proportional to the rate of change of magnetic flux linkage. Operating at higher frequencies or optimizing resonant tuning can therefore improve voltage transfer and efficiency.

Overall, the results indicate that system performance can be significantly improved through better coil alignment, optimized operating frequency, and enhanced coupling efficiency.

The observed low efficiency (approximately 4.5%) in this experiment suggests that magnetic coupling between the coils is relatively weak, possibly due to air-gap losses or imperfect resonance matching. Future improvements should focus on optimizing coil geometry and tuning both sides of the circuit to resonate at the same frequency.

#### V. Conclusion

The hardware implementation of the Wireless Power Transfer (WPT) system for electric vehicles (EVs) was successfully completed. High-rating power electronics and proper resonance are crucial for maximizing efficiency. Our system transfers electricity over a 5–10 cm gap with lower energy efficiency than commercial systems (85–92 percent).

Wireless charging is gaining global adoption—for example, taxis in Norway charge in 6–8 minutes, and buses in South Korea charge while driving. However, high costs, limited power infrastructure, and safety considerations, including electromagnetic interference (EMI), pose challenges for countries like Nepal. Future improvements should focus on precise coil alignment, advanced circuit designs such as LCC, matching high-efficiency operating frequencies (e.g., 85 kHz), and considering scalability for multiple EVs. These steps can make wireless EV charging safer, more energy-efficient, and practical worldwide.

#### Acknowledgment

We, the authors, would like to express our sincere gratitude to all the individuals and organizations who provided their invaluable support and guidance throughout the course of this research. Our heartfelt appreciation goes to **Kathmandu Engineering College** for providing us with the ideal platform and environment to carry out, present, and publish our work. The opportunity offered by KEC not only fostered our academic and technical growth but also encouraged us toward the successful completion and publication of this research.

#### References

- [1] N. H. Solouma, H. B. Kassahun, A. S. Alsharafi, A. Syed, M. R. Gardner, and S. S. Alsharafi, "An Efficient Design of Inductive Transmitter and Receiver Coils for Wireless Power Transmission," *Electronics*, vol. 12, no. 3, p. 564, 2023.
- [2] C. Yahaya, S. F. S. Adnan, M. Kassim, R. Ab Rahman, and M. F. Bin Rusdi, "Analysis of wireless power transfer on the inductive coupling resonant," *Indonesian Journal of Electrical Engineering and Computer Science*, vol. 12, no. 2, pp. 592-599, 2018.
- [3] T. S. H. and R. M. H. Sagolsem Kripachariya Singh, "Wireless Transmission of Electrical Power Over review of Recent Research & Development," *Int. J. Comput. Electr. Eng.*, vol. 4, no. 2, pp. 207–211, 2012
- [4] D. M. S. R. YIN QUAN TEO, "Wireless Power Transmission in the Smart Home," vol. 2010.
- [5] F.F. Almutairi, "Classification: Public Wireless Power Transfer: A Critical Analysis of Past Endeavors and Future Prospects," vol. 2024
- [6] Carvalho, N. (2017). Europe and the Future for WPT: European Contributions to Wireless Power Transfer Technology, *IEEE Microwave Magazine*, 18(4), pp 56-87. <https://doi.org/10.1109/MMM.2017.2680078>

- [7] Jawad et al. (2017). Opportunities and Challenges for Near-Field Wireless Power Transfer: A Review, *energies journal*, 10(7), pp 1-8. <https://doi.org/10.3390/en10071022>
- [8] Sun, T. Xie, X. and Wang, Z. (2013). Design challenges of the wireless power transfer for medical microsystems," *IEEE International Wireless Symposium (IWS)*, Beijing, China
- [9] Detka K, Górecki K. Wireless Power Transfer—A Review. *Energies journal*. 2022; 15(19), pp. 14-36. <https://doi.org/10.3390/en15197236>. [8] Shan et al. (2022). Wireless power transfer system with enhanced efficiency by using frequency reconfigurable metamaterial, *springer nature*, 2(1) <https://www.nature.com/articles/s41598-021-03570-8>
- [10] Zambak et al. (2014). Wireless power transfer by using solar energy, *School of Electrical System Engineering, University Malaysia Perlis*, 12(3), pp 38-46. <http://doi.org/10.12928/telkomnika.v12i3.93>
- [11] Thukral, M.K. Design and Simulink implementation of electrical vehicle charging using wireless power transfer technology. In *Optical and Wireless Technologies*; Springer: Singapore, 2020
- [12] Dashora, H. K. (n.d.). *Dynamic Wireless Charging of Electric Vehicle* (PhD thesis). University of Padova.
- [13] Al-Atraqchi, Z. A. (2020). *Simulation and Implementation of Wireless Power Transfer System* (M.Sc. thesis). University of Ninevah.
- [14] Lopes, P. M. C. (2021). *Wireless Power Transfer System For Electric Vehicle Charging* (Master's thesis). Universidade de Lisboa.